

Portable and Lightweight Signal Processing Approach for sEMG-Based Human–Machine Interaction in Robotic Hands

Ngoc-Khoat Nguyen

Faculty of Control and Automation, Electric Power University, Hanoi, Vietnam

Abstract—Surface electromyography (sEMG) presents a viable biosignal for the control of robotic prosthetic hands, as it directly correlates with underlying muscle activity. This study introduces an efficient, computationally lightweight signal processing methodology designed for real-time embedded systems. The proposed methodology comprises a preprocessing pipeline, incorporating bandpass and notch filtering, followed by segmentation via overlapping sliding windows. Time-domain features, specifically Mean Absolute Value (MAV), Zero Crossing (ZC), Waveform Length (WL), Slope Sign Change (SSC), and Variance (VAR), are extracted to characterize relevant muscular activation patterns. By prioritizing computational efficiency and embedded system feasibility, this method establishes a practical framework for user intent recognition and real-time control of wearable robotic hands, particularly within assistive and rehabilitative applications. The experimental findings clearly indicate that the extracted features effectively differentiate between various hand gestures, allowing for accurate, real-time control of the wearable robotic hand. The system's high responsiveness, low latency, and resilience to noise underscore its suitability for assistive and rehabilitative applications. With its focus on computational simplicity and feasibility for embedded implementation, the proposed method provides a practical basis for recognizing user intent in human-machine interaction systems.

Keywords—sEMG; myo-prosthesis; myosignals; human–prosthesis interface; signal processing

I. INTRODUCTION

The upper limb plays a crucial role to a wide spectrum of daily human activities, encompassing both intricate manipulations, such as object grasping and writing, and complex movements requiring multi-joint coordination [1]. Anatomically, the upper limb comprises distinct segments—the hand, forearm, and upper arm—functioning through the coordinated interaction of the central nervous system, musculoskeletal system, and environmental sensory feedback. This inherent complexity presents substantial challenges in the design of artificial prosthetic systems, particularly robotic hands, where dexterity, precision, and user-intent-driven control are paramount. The partial or complete loss of an upper limb, resulting from trauma, disease, or other etiologies, can significantly impair an individual's quality of life, self-care capabilities, and social integration.

In recent years, a growing number of studies have explored the use of bio-signals originating from the human body to control prosthetic limbs, due to their rich information content regarding motor intentions. Among these, electromyography

(EMG) signals have been extensively investigated for their ability to reflect muscle activity [2]–[4]. However, raw surface EMG (sEMG) signals cannot be directly used for motion recognition or robotic control due to their inherent spatial and temporal complexity [5]. Factors such as electrode displacement, muscle fatigue, variability in contraction intensity, and inter-subject differences contribute to reduced accuracy and repeatability in EMG-based control systems [6], [7].

Various techniques have been employed to process EMG signals, yet the core processing pipeline remains largely consistent. Initially, EMG signals are amplified and filtered after acquisition. This is particularly crucial in clinical or rehabilitation scenarios where residual muscle strength may be weak, resulting in significantly lower sEMG amplitudes compared to those in healthy individuals. Proper filter and amplifier design not only improves the signal-to-noise ratio (SNR) but also enhances the reliability of extracting relevant motor information from the signal [8].

Following preprocessing, sEMG signals are segmented using time windows, dividing the continuous data into short, fixed-length segments. Overlapping windowing is the most commonly adopted method, with the choice of window size and stride length being critical for balancing latency and accuracy. Each segment is then used to extract features that characterize muscle activity over the corresponding time interval [9].

Extracted features can belong to the time domain (TD), frequency domain (FD), or time–frequency domain (TFD). Time-domain features are directly calculated from raw sEMG signals and are functions of time [10]. TD features are widely favored due to their simplicity and computational efficiency, making them well-suited for real-time control systems. Common TD features include Mean Absolute Value (MAV), Zero Crossings (ZC), Waveform Length (WL), Slope Sign Changes (SSC), and Variance (VAR), which reflect the intensity, shape, and variation of the EMG signal. These features serve as useful inputs for subsequent classification or control stages, and have been extensively studied for EMG recognition tasks [11]–[13]. For instance, in [11], six TD features (MAV, WL, RMS, AR, ZC, SSC) were used to classify seven hand gestures, with Support Vector Machines (SVM) achieving the highest accuracy (95.26 per cent) compared to LDA (92.58 per cent) and k-NN (86.41 per cent).

In addition to TD features, FD features also play a key role in describing the spectral properties of EMG signals [14]. By

applying spectral analysis techniques such as the Fast Fourier Transform (FFT), indicators such as spectral energy, Mean Frequency (MNF), and Median Frequency (MDF) can be extracted. FD features are commonly used in fatigue analysis or combined with TD features to improve classification performance [13]. Time–frequency domain transformations such as the Short-Time Fourier Transform (STFT), FFT, and wavelet transforms preserve both TD and FD characteristics of the signal. However, TFD-based methods remain relatively underexplored due to their complexity and limited interpretability [8].

After extracting EMG features from one or more domains, the next step is to classify or recognize the user's intended movements. This is a crucial stage that translates physiological signals into control commands for robotic hands. Numerous machine learning algorithms have been successfully employed for EMG classification, ranging from traditional methods such as k-Nearest Neighbors (k-NN) [15], Linear Discriminant Analysis (LDA) [16], [23], and Support Vector Machines (SVM) [11], [17]–[19], to advanced deep learning models such as Convolutional Neural Networks (CNN) [20], [21] and Recurrent Neural Networks (RNN) [22]. Simpler models like LDA and SVM are often preferred in real-time systems due to their low computational overhead and effectiveness with linearly or near-linearly separable features. On the other hand, deep learning models can directly learn representations from raw or time–frequency-transformed data such as spectrograms or scalograms, yielding higher accuracy at the cost of increased computational requirements.

This study focuses on the preprocessing and feature extraction stages of sEMG signals as a foundation for recognizing user intent in robotic hand control. The signal undergoes preprocessing steps, including high-pass filtering, notch filtering, and low-pass filtering, to reduce noise and normalize data. Subsequently, time-domain features such as MAV, ZC, WL, SSC, and VAR are extracted using a sliding window technique, providing the necessary inputs for later classification and control stages.

The main contribution of this paper is the proposal and evaluation of a simple yet effective sEMG signal processing method that can be integrated into real-time embedded systems such as microcontrollers or wearable robotic control devices. This research lays the groundwork for incorporating machine learning techniques that enable more intuitive and adaptive robotic control. Additionally, it contributes to the development of user-intent-based control systems for robotic hands, targeting applications in rehabilitation and assistive technologies.

The subsequent sections are organized as follows: Section II covers the materials and methods used for sEMG signal acquisition and processing, detailing the signal conditioning and feature extraction steps. Section III explains the integration of the proposed method for real-time robotic hand control and describes the validation experiments performed across diverse hand gestures. Section IV presents a discussion centered on the results of these experiments, including an analysis of the

proposed method's benefits and drawbacks. Lastly, Section V summarizes the key findings and identifies potential avenues for future work.

II. MATERIALS AND METHODS

A. Signal Analysis

1) *sEMG acquisition hardware*: In this study, the surface electromyography (sEMG) sensor module DFRobot – OYMotion (Product Code: SEN0240) was employed to acquire electromyographic signals generated by muscle contractions of the user. The overall structure of the SEN0240 sensor module is illustrated in Fig. 1. This analog sEMG module, co-developed by DFRobot and OYMotion, integrates essential functional blocks including signal amplification, noise filtering, and primary signal conditioning.

One of the most notable advantages of this module is its capability to operate with dry metal electrodes, eliminating the need for conductive gel typically required by conventional medical electrodes. This feature significantly simplifies the setup process, enhances durability, and improves user convenience, particularly in non-invasive human–machine interaction (HMI) applications. The use of dry electrodes allows for flexible deployment on both static and dynamic muscle regions while maintaining reliable signal quality.

The sensor is capable of amplifying small sEMG signals in the range of ± 1.5 mV up to 1000 times. It utilizes differential input combined with an integrated analog filtering stage to effectively suppress noise, particularly power line interference at 50/60 Hz. The sensor operates optimally within a frequency range of 20 Hz to 500 Hz, which corresponds to the primary spectral band of sEMG signals. The output is provided as an analog voltage signal with a reference level of 1.5 V and a swing range from 0 to 3.0 V, making it well-suited for digitization via analog-to-digital converters (ADCs) in microcontroller-based embedded systems.

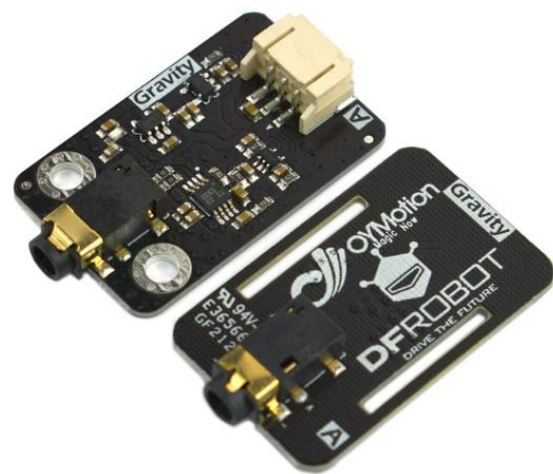


Fig. 1. SEN0240 analog EMG sensor by OYMOTION [24].

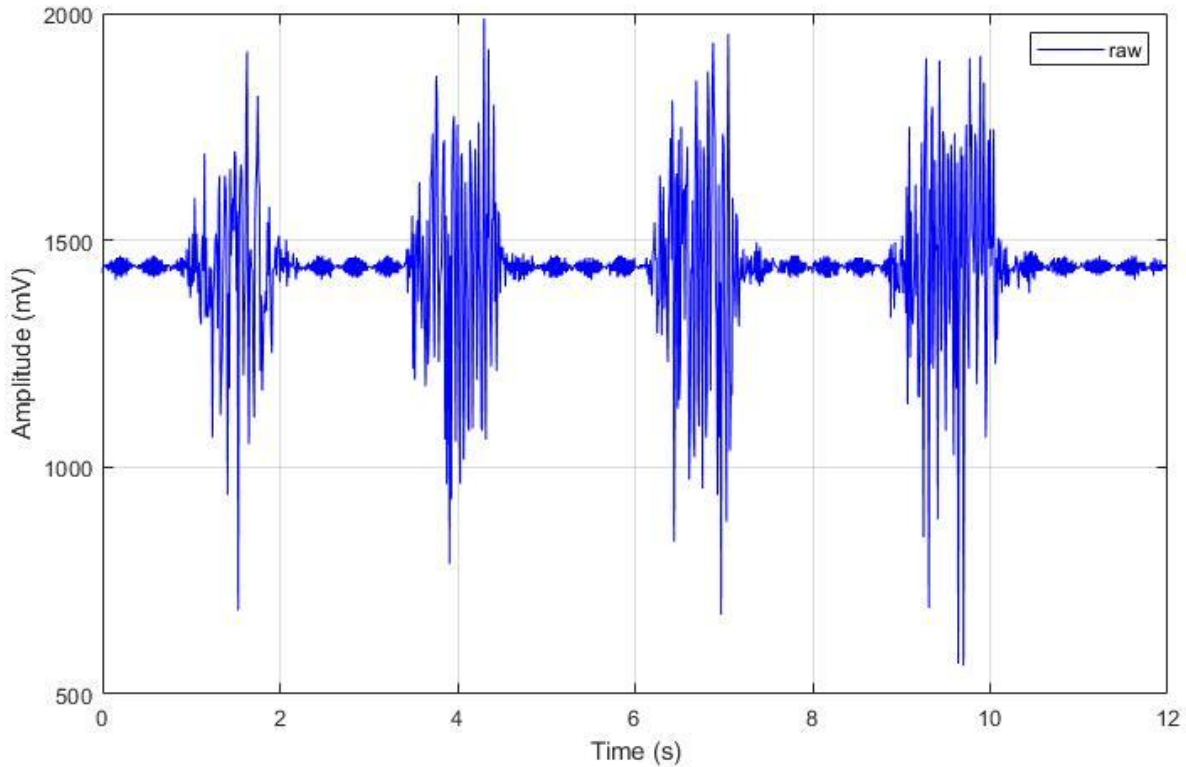


Fig. 2. An illustration of a raw sEMG signal.

Fig. 2 illustrates a raw sEMG signal acquired from the SEN0240 sensor using a 10-bit ADC. The signal was sampled at a frequency of 1000 Hz. The output amplitude fluctuates within the range of approximately 500 mV to 2000 mV, with an average baseline (offset) value around 1.5 V (1500 mV), consistent with the sensor's technical specifications. The signal clearly demonstrates alternating phases of muscle contraction and relaxation, characterized by high-amplitude fluctuations during active periods and near-flat regions during rest. Notably, strong muscle contractions occur at approximately 1.5s, 4.5s, 7s, and 9.5s, with signal amplitudes spiking significantly above the baseline level. During the resting intervals, the signal oscillates mildly around 1.5 V, indicating minimal muscle activity. The presence of power line interference (50 Hz) or high-frequency noise components is noticeable, particularly in the low-activity segments.

2) *Signal preprocessing*: The surface electromyography (sEMG) signal was acquired from the SEN0240 sensor using a three-electrode configuration: two electrodes placed over the muscle and one reference (GND) electrode. The output signal is in the form of an analog voltage within the 0–3.0 V range, with a baseline level of approximately 1.5 V. The amplitude fluctuations of the signal reflect the level of muscle activity.

A sampling frequency of 1000 Hz was selected, which is suitable for the effective bandwidth of sEMG signals (20 to 500 Hz) [25], [26] and satisfies the Nyquist sampling theorem to prevent aliasing. After acquisition, the signal values were

converted from raw ADC units to millivolts (mV) to facilitate further processing.

Raw sEMG signals are often contaminated by various noise sources, such as power line interference during acquisition and poor electrode-skin contact, which introduces additional artifacts [27]. Therefore, a signal pre-processing stage is essential. De Luca et al. [28] emphasized the use of high-pass filters to eliminate low-frequency noise, recommending a cutoff frequency of 20 Hz for natural movements and higher values for intense physical activity. Conversely, a low-pass filter with a cutoff frequency between 400 and 500 Hz is recommended. One of the most widely adopted solutions for EMG signal filtering is the use of a Butterworth band-pass filter with a typical passband ranging from 20 to 450 Hz.

In this study, the sEMG signal was pre-processed using a three-stage filtering approach. First, a high-pass filter with a cutoff frequency of 20 Hz was applied to remove low-frequency drift and DC offset while preserving relevant muscle activity components. Next, an IIR notch filter centered at 50 Hz was used to suppress power line interference, which typically appears as a dominant peak in the EMG frequency spectrum [29]. Finally, a low-pass filter with a cutoff frequency of 450 Hz was employed to eliminate high-frequency noise, including impulsive and RF interference. Both the high-pass and low-pass filters were implemented as second-order Butterworth filters to ensure a flat frequency response in the passband and minimal signal distortion. The filtering process was performed using the zero-phase filtfilt method to avoid phase delay.

3) *Overlapped sliding window segmentation*: The sEMG signal is segmented into smaller portions to facilitate time-domain feature extraction. The choice of segment length must be carefully considered: overly long segments may increase computational load, whereas segments that are too short can result in inaccurate feature extraction. In real-time applications in particular, segment lengths exceeding 200 milliseconds often require the use of overlapping techniques to ensure continuity and responsiveness in system feedback [30].

This method divides the signal into fixed-length windows (w), with each window being shifted by a smaller step size (s). This results in overlapping segments, meaning that a single signal sample may appear in multiple consecutive windows. The window length (w) determines the amount of EMG data used for feature extraction, while the step size (s) defines the temporal distance between windows and controls the sliding rate. A smaller step size leads to increased overlap and provides more data for analysis [37]. Selecting an appropriate window and step size is a crucial factor. Larger window sizes allow for more comprehensive information capture and lower variability in extracted features. However, excessively large windows can introduce perceptible delays, which may negatively impact the user experience when using assistive devices. Therefore, as suggested in [38], the optimal window length is typically in the range of 150 ms to 250 ms.

In this study, the window size (w) is set to 200 ms, and the step size (s) is set to 50 ms, as illustrated in Fig. 3. With a sampling frequency of 1 kHz, each window corresponds to 200 samples. As each window shifts by 50 samples, there is a 75 per cent overlap between consecutive windows.

This sliding window-based segmentation effectively captures the temporal characteristics of the sEMG signal, thereby enhancing the accuracy and robustness of the gesture recognition system [36].

4) *Feature extraction*: The sliding window-based signal analysis method not only ensures the ability to continuously monitor muscle activity over time but also facilitates the subsequent feature extraction stage. The segmented signal obtained through this technique exhibits a stable format and well-defined structure, which enhances the accuracy of feature computation and meets the real-time requirements of human-machine interactive robotic control systems.

Extracted features can be categorized into time-domain, frequency-domain, or time-frequency domain features [31]-[34]. Frequency-domain features help identify the frequency components of muscle activity, providing insights into muscle activation levels and the ability to suppress noise. The signal is transformed into the frequency domain using the Discrete Fourier Transform (FFT). Commonly used frequency-domain features include Mean Frequency (MNF), Median Frequency (MDF), Mean Power Frequency (MNP), Peak Frequency (PKF), and Total Power (TTP) [Phinyomark, Yinfeng]. The combination of information from both time and frequency domains is defined as time-frequency features. Common

techniques used in this category include Discrete Wavelet Transform (DWT), Short-Time Fourier Transform (STFT), and Wavelet Packet Energy [34].

Frequency-domain features are often used to study muscle fatigue or in motor unit analysis; however, they are generally not suitable for EMG signal classification [32], [33]. In addition, the high computational load may pose challenges for real-time control applications. Time-domain feature extraction, by contrast, is a widely adopted and effective approach for characterizing sEMG signals with low computational complexity, making it well-suited for real-time control systems. These features are directly derived from the amplitude values of the signal within each sliding window.

In this study, the selected time-domain feature includes:

a) *Mean absolute value (MAV)*: The average of the absolute values of the EMG signal within a window, representing the intensity of muscle activity.

$$MAV = \frac{1}{N} \sum_{i=1}^N |x_i| \quad (1)$$

b) *Waveform length (WL)*: The cumulative length of the EMG signal waveform within a segment, representing the signal's variability and complexity [35].

$$WL = \sum_{i=1}^{N-1} |x_{i+1} - x_i| \quad (2)$$

c) *Variance (VAR)*: The statistical dispersion of the EMG signal within a segment, reflecting its energy level.

$$VAR = \frac{1}{N-1} \sum_{i=1}^N x_i^2 \quad (3)$$

d) *Zero crossing (ZC)*: The number of times the EMG signal amplitude crosses the zero-voltage level within a segment. To avoid counting low-voltage fluctuations or background noise, a threshold condition is implemented. The calculation is defined as:

$$ZC = \sum_{i=1}^{N-1} [\text{sgn}(x_i \times x_{i+1}) \cap |x_i - x_{i+1}| \geq \text{threshold}] \quad (4)$$

$$\text{sgn}(x) = 1, \text{ if } x \geq \text{threshold}$$

$$\text{sgn}(x) = 0, \text{ otherwise}$$

e) *Slope Sign changes (SSC)*: This feature is used to represent the frequency-related information of the EMG signal. It counts the number of times the slope of the signal changes sign, which helps detect abrupt variations and transitions in the signal.

$$SSC = \sum_{i=1}^{N-1} [f[(x_i - x_{i-1}) \times (x_i - x_{i-1})]] \quad (5)$$

$$f(x) = 1, \text{ if } x \geq \text{threshold}$$

$$f(x) = 0, \text{ otherwise}$$

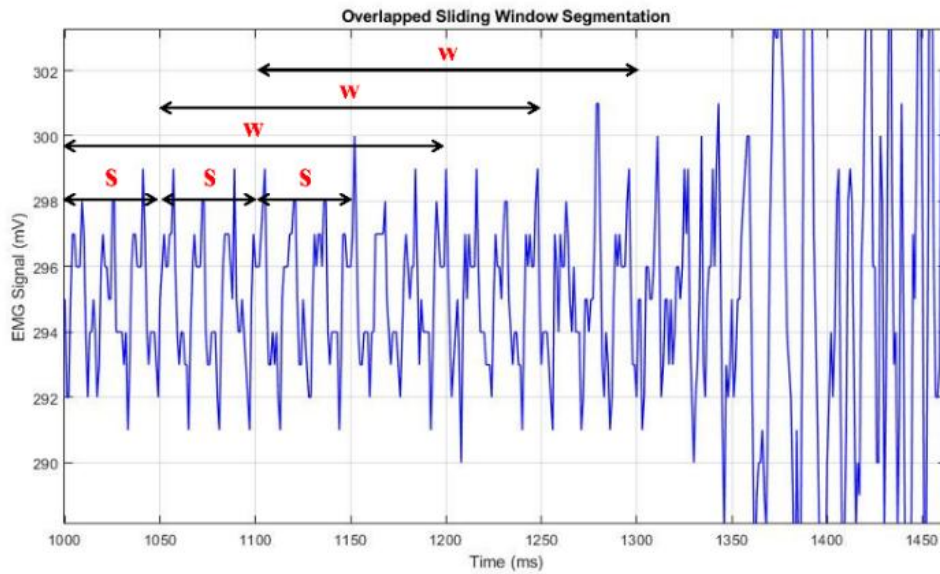


Fig. 3. Window segmentation of the sEMG signal.

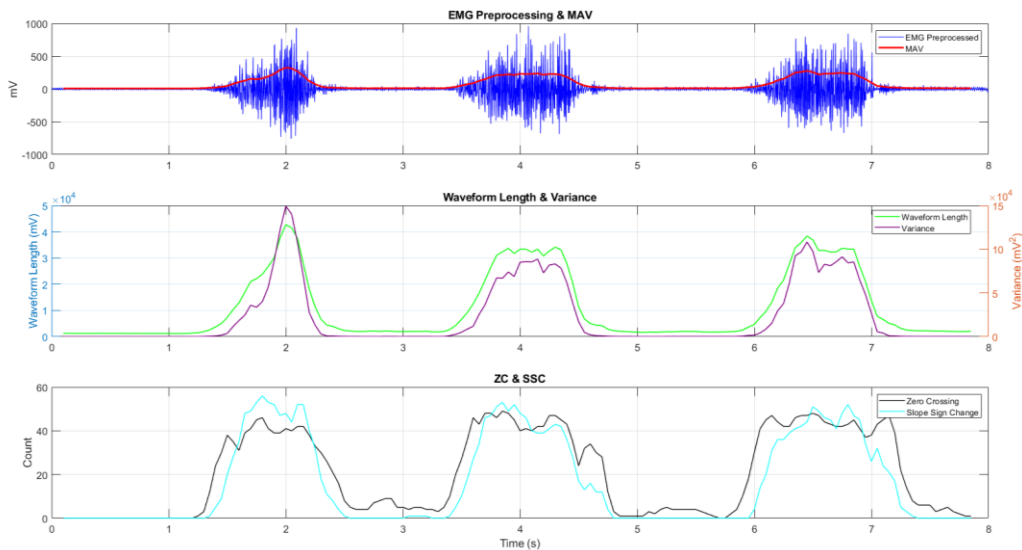


Fig. 4. An example of an EMG signal recorded with MAV, WL, VAR, ZC and SSC features.

During the sEMG signal analysis as shown in Fig. 4, time-domain features are extracted to characterize muscle activity. The Mean Absolute Value (MAV) reflects the level of muscle contraction through the signal amplitude. Waveform Length (WL) and Variance (VAR) indicate the signal's complexity and variability, while Zero Crossing (ZC) and Slope Sign Change (SSC) provide insights into the frequency of waveform transitions. These features enable clear discrimination between rest and contraction states, forming a foundation for motion recognition and robotic control.

B. Application in Artificial Hand Control

1) *Sensor location*: The placement of EMG electrodes plays a critical role in distinguishing the performance across

different finger movement patterns. Achieving this requires a solid understanding of the underlying muscular structure responsible for finger control, particularly when selecting optimal sEMG electrode positions. Within the forearm region, two major muscle groups are primarily involved in finger movement control: the flexor muscles and the extensor muscles. These muscle groups are situated on both sides of the wrist and run along the length of the forearm.

The flexor muscles, located on the anterior side of the forearm, such as the Flexor Digitorum Profundus (FDP) and Flexor Digitorum Superficialis (FDS), are responsible for flexing the wrist and fingers. In contrast, the extensor muscles, situated on the posterior side, including the Extensor Digitorum

(or Extensor Digitorum Communis – EDC) and Extensor Digiti Minimi (EDM), control the extension of these joints. These two muscle groups operate in opposition: when one contracts, the other relaxes. Therefore, to effectively capture EMG signals associated with finger activity, it is essential to position sEMG electrodes over both the flexor and extensor muscle regions.

Fig. 5 illustrates the electrode placement strategy. Electrode position 1 targets the activity of the ring and little fingers; position 2 corresponds to the index and middle fingers; and position 3 captures movements of the thumb. The electrodes are aligned centrally along the muscle fibers and spaced approximately 2.5 cm apart to ensure optimal signal acquisition.

2) *Artificial hand control*: Fig. 6 illustrates the overall control diagram of the artificial hand system based on surface electromyography (sEMG) signals. The system utilizes three sEMG sensors placed on the user's arm to acquire bioelectrical signals generated by muscle activity. These signals are preprocessed to remove noise and normalized before feature extraction. The extracted features are then classified to identify the user's intended motion. The classification results are used as input for the controller to actuate the robotic hand accordingly. A human-machine interface (HMI) is integrated to visualize sEMG signals and system status in real-time. Additionally, the system supports communication with a computer for monitoring, data analysis, and parameter adjustment.

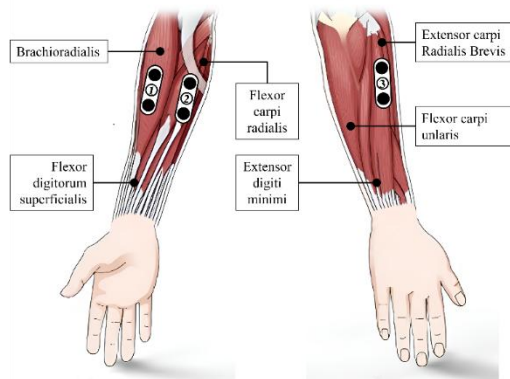


Fig. 5. Human hand muscle structure and electrode placement.

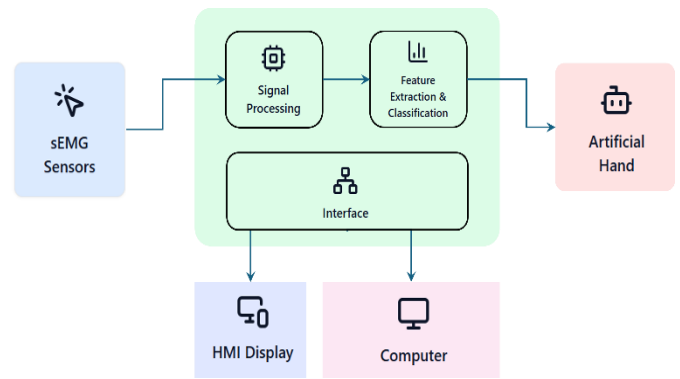


Fig. 6. The control system overview diagram.

III. EXPERIMENTAL RESULTS

To evaluate the effectiveness of the proposed EMG-based control system, both signal processing results and real-time robotic hand responses were analyzed. Fig. 7 illustrates the EMG signals from three channels, along with the extracted features: Mean Absolute Value (MAV), Variance (VAR), and Waveform Length (WL). These features were computed in real-time over a sliding window and are visualized to correlate with the four distinct muscle activation segments corresponding to different gestures.

The MAV feature showed consistent performance in highlighting the onset and duration of muscle activation across all channels. On the other hand, VAR and WL provided additional sensitivity in distinguishing gestures with similar EMG amplitudes but different signal complexities. The combination of these three features thus offers a robust representation of muscle activity, suitable for classifying and interpreting user intentions.

Fig. 8 demonstrates the practical implementation of the control system, where each user gesture (e.g., wrist extension, flexion, or grasping motion) was successfully translated into the corresponding movement of the robotic hand. The robotic hand responded in real-time with clear alignment to the user's intended actions.

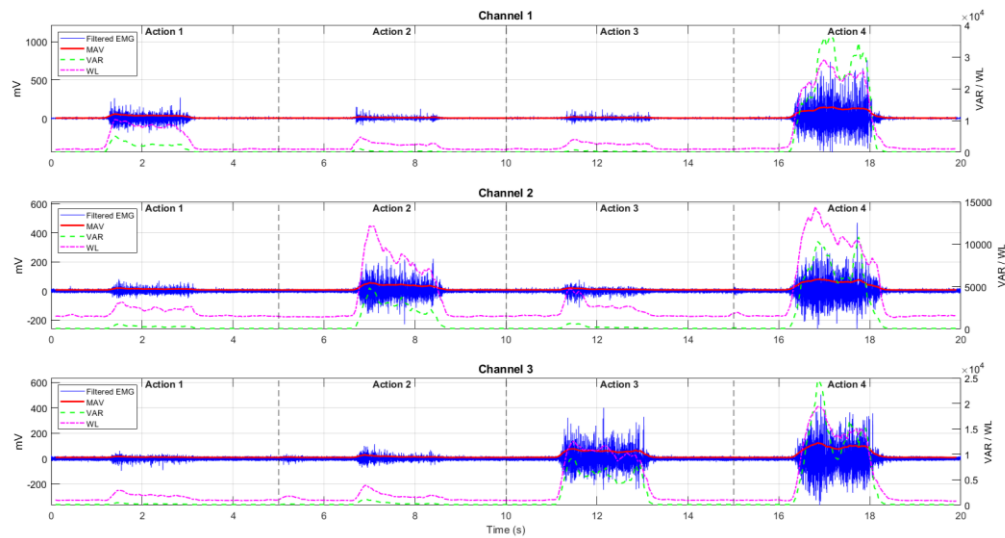


Fig. 7. EMG signals and extracted features during different hand motions.

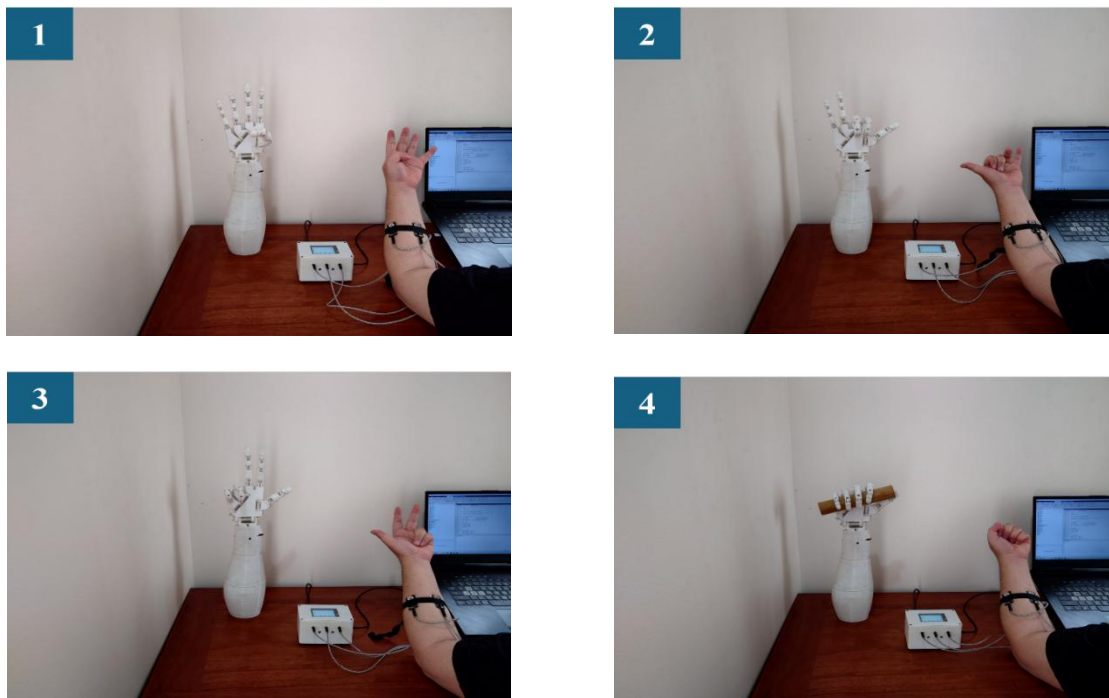


Fig. 8. Real-time EMG-based control of a prosthetic hand using four distinct hand gestures.

IV. DISCUSSIONS

The experimental results illustrated in the previous section confirm that the EMG signals acquired from the forearm can effectively control a wearable robotic hand in real time. The proposed system offers low latency and high responsiveness, critical for natural human-machine interaction.

Furthermore, the feature extraction and segmentation pipeline proved reliable in isolating intentional movement from resting or noise-dominant periods. Although the system currently operates on predefined gestures, it provides a foundation for further development involving real-time

classification algorithms such as Support Vector Machines or Neural Networks.

Despite the promising results, this study has some limitations. First, the system currently relies on a limited number of predefined hand gestures, which restricts its general applicability. Second, the experiment was conducted with a small number of participants under controlled conditions, which may not fully represent real-world variability in sEMG signals across different users or usage scenarios. Additionally, although the proposed method is optimized for embedded implementation, further evaluation on various hardware

platforms is needed to assess performance consistency. Addressing these limitations will be a key focus in future work.

V. CONCLUSION

This study presents a preliminary investigation into the processing of surface electromyography (sEMG) signals for the control of wearable robotic hand systems. A foundational signal processing framework, suitable for real-time applications, was developed, encompassing filtering, window-based segmentation, and the extraction of relevant time-domain features, including Mean Absolute Value (MAV), Waveform Length (WL), Variance (VAR), Zero Crossing (ZC), and Slope Sign Changes (SSC).

The implementation of sliding window segmentation and feature extraction from strategically positioned sEMG electrodes over both flexor and extensor muscles demonstrated efficacy in capturing muscle activity associated with finger movements. These extracted features serve as input vectors for subsequent classification and control algorithms.

This work constitutes an initial phase in the development of a comprehensive human-machine interface. It establishes a basis for future research focused on the integration of advanced classification algorithms, such as Support Vector Machines (SVM), k-Nearest Neighbors (k-NN), or deep learning methodologies, for accurate gesture recognition and adaptive robotic hand control. The findings of this study are anticipated to contribute to the advancement of intuitive, responsive, and user-centered assistive robotic systems, particularly for rehabilitation and prosthetic applications.

ACKNOWLEDGMENT

This work is funded by Electric Power University, following University Project in 2025. The author wishes to acknowledge Mr. Nguyen Van Kien, B.A., for his support in validating the experimental results presented herein.

REFERENCES

- [1] T. Feix, J. Romero, H. -B. Schmiemayer, A. M. Dollar and D. Kragic, "The GRASP Taxonomy of Human Grasp Types," in IEEE Transactions on Human-Machine Systems, vol. 46, no. 1, pp. 66-77, Feb. 2016, doi: 10.1109/THMS.2015.2470657.
- [2] J. F. Castruita-López, M. Aviles, D. C. Toledo-Pérez, I. Macías-Socarrás, J. Rodríguez-Reséndiz, "Electromyography Signals in Embedded Systems: A Review of Processing and Classification Techniques", Biomimetics, 10(3), 166, 2025, doi: 10.3390/biomimetics10030166
- [3] Z. Mingde; C. S. Michael, S. E. Michael, "Surface electromyography as a natural human-machine interface: a review", IEEE Sensors Journal, 22.10: 9198-9214, 2022, doi: 10.1109/JSEN.2022.3165988.
- [4] H. Mo, et al, "Inference of upcoming human grasp using emg during reach-to-grasp movement", Frontiers in Neuroscience, 16: 849991, 2022, doi: 10.3389/fnins.2022.849991.
- [5] A. Phinyomark, E. Scheme, "EMG pattern recognition in the era of big data and deep learning", Big Data and Cognitive Computing, 2(3), 21, 2018, doi: 10.3390/bdcc2030021.
- [6] N. Parajuli, et. al, "Real-time EMG based pattern recognition control for hand prostheses: A review on existing methods, challenges and future implementation", Sensors, 19(20), 4596, 2019, doi: 10.3390/s19204596.
- [7] C. Ahmadzadeh, M. Khoshnam, and C. Menon, "Human machine interfaces in upper-limb prosthesis control: A survey of techniques for preprocessing and processing of biosignals", IEEE Signal Processing Magazine, 38(4), 12-22, 2021, doi: 10.1109/MSP.2021.3057042.
- [8] T. Song, Z. Yan, S. Guo, Y. Li, X. Li, and F. Xi, "Review of sEMG for Robot Control: Techniques and Applications", Applied Sciences, 13(17), 9546, 2023. doi: 10.3390/app13179546
- [9] W. Li, P. Shi, and H. Yu, "Gesture recognition using surface electromyography and deep learning for prostheses hand: state-of-the-art, challenges, and future", Frontiers in neuroscience, 15, 621885, 2021, doi: 10.3389/fnins.2021.621885.
- [10] J. Liu, "Adaptive myoelectric pattern recognition toward improved multifunctional prosthesis control", Medical engineering & physics, 37(4), 424-430, 2015, doi: 10.1016/j.medengphy.2015.02.005.
- [11] H.F. Hassan, S. J. Abou-Loukh, and I. K. Ibraheem, "Teleoperated robotic arm movement using electromyography signal with wearable Myo armband", Journal of King Saud University-Engineering Sciences, 32(6), 378-387, 2020, doi: 10.1016/j.jksues.2019.05.001.
- [12] O. Kerdjadj, K. Amara, F. Harizi and H. Boumidja, "Implementing Hand Gesture Recognition Using EMG on the Zynq Circuit," in IEEE Sensors Journal, vol. 23, no. 9, pp. 10054-10061, 1 May1, 2023, doi: 10.1109/JSEN.2023.3259150.
- [13] H. A. Javaid, et al, "Classification of Hand Movements Using MYO Armband on an Embedded Platform", Electronics, 10(11), 1322, 2021, doi: 10.3390/electronics10111322
- [14] E. Scheme, et al. "Motion normalized proportional control for improved pattern recognition-based myoelectric control", IEEE Transactions on Neural Systems and Rehabilitation Engineering, 22(1), 149-157, 2013, doi: 10.1109/TNSRE.2013.2247421.
- [15] T. Triwiyanto, S. Luthfiah, W. Caesarendra, and A. A. Ahmed, "Implementation of Supervised Machine Learning on Embedded Raspberry Pi System to Recognize Hand Motion as Preliminary Study for Smart Prosthetic Hand", Indonesian Journal of Electrical Engineering and Informatics (IJEED), 11(3), 685-699, 2023, doi: 10.52549/ijeei.v11i3.4397.
- [16] R. D. Babu, S. S. Adithya, and M. Dhanalakshmi, M. "Design and development of an EMG controlled transfemoral prosthesis", Measurement: Sensors, 36, 101399, 2024, doi: 10.1016/j.measen.2024.101399.
- [17] A. Grattarola, et al, "Grasp Pattern Recognition Using Surface Electromyography Signals and Bayesian-Optimized Support Vector Machines for Low-Cost Hand Prostheses", Applied Sciences, 15(3), 1062, 2025, doi: 10.3390/app15031062
- [18] T. Prabhavathy, V. K. Elumalai, and E. Balaji, "Hand gesture classification framework leveraging the entropy features from sEMG signals and VMD augmented multi-class SVM", Expert Systems with Applications, 238, 121972, 2024, doi: 10.1016/j.eswa.2023.121972.
- [19] A. Yilmaz, et al, "Hand Movement Classification with Four Channel EMG Signals for Underactuated Hand Prosthesis Test Platform", In 2024 32nd Signal Processing and Communications Applications Conference (SIU) (pp. 1-4). IEEE, doi: 10.1109/siu61531.2024.10600778
- [20] Z. C. Mhiriz, M. Bourhaleb, and M. Rahmoune, "Leveraging Machine Learning for Signal Processing in Surface Electromyography (sEMG) for Prosthetic Control", In International Conference on Digital Technologies and Applications (pp. 107-116). Cham: Springer Nature Switzerland, 2024, doi: 10.1007/978-3-031-68650-4_11
- [21] F. Laganà, D. Praticcò, G. Angiulli, G. Oliva, S. A. Pullano, M. Versaci, and F. L. Foresta, "Development of an Integrated System of sEMG Signal Acquisition, Processing, and Analysis with AI Techniques", Signals, 5(3), 476-493, 2024, doi: 10.3390/signals5030025
- [22] A. T. Nguyen, et al "A portable, self-contained neuroprosthetic hand with deep learning-based finger control", Journal of neural engineering, 18(5), 056051, 2021, doi: 10.1088/1741-2552/ac2a8d
- [23] S. Pancholi, and A. M. Joshi, "Electromyography-based hand gesture recognition system for upper limb amputees", IEEE Sensors Letters, 3(3), 1-4, 2019, doi: 10.1109/LSENS.2019.2898257.
- [24] SEN0204 Analog EMG Sensor by OYMotion, doi: https://wiki.dfrobot.com/Analog_EMG_Sensor_by_OYMotion_SKU_S_EN0204
- [25] M. S. H. Majid et al, "EMG feature extractions for upper-limb functional movement during rehabilitation". In 2018 international conference on intelligent informatics and biomedical sciences (ICIIBMS) (Vol. 3, pp. 314-320), 2018, doi: 10.1109/ICIIBMS.2018.8549932.

- [26] G. Li, L. Yu, and Y. Geng, "Conditioning and sampling issues of EMG signals in motion recognition of multifunctional myoelectric prostheses", *Annals of biomedical engineering*, 39, 1779-1787, 2011, doi: 10.1007/s10439-011-0265-x.
- [27] S. Bisi, L. D. Luca, B. Shrestha, Z. Yang, and V. Gandhi, "Development of an EMG-controlled mobile robot", *Robotics*, 7(3), 36, 2018, doi: 10.3390/robotics7030036.
- [28] C. J. De Luca, et al "Filtering the surface EMG signal: Movement artifact and baseline noise contamination", *Journal of biomechanics*, 43(8), 1573-1579, 2010, doi: 10.1016/j.jbiomech.2010.01.027.
- [29] R. Ahmed, R. Halder, M. Uddin, P. C. Mondal and A. K. Karmaker, "Prosthetic Arm Control Using Electromyography (EMG) Signal," 2018 International Conference on Advancement in Electrical and Electronic Engineering (ICAEEE), Gazipur, Bangladesh, 2018, pp. 1-4, doi: 10.1109/ICAEEE.2018.8642968.
- [30] D. Karabulut, et al, "Comparative evaluation of EMG signal features for myoelectric controlled human arm prosthetics", *Biocybernetics and Biomedical Engineering*, 37(2), 326-335, 2017, doi: 10.1016/j.bbe.2017.03.001.
- [31] M. D. Olmo, and D. Rosario, "EMG Characterization and Processing in Production Engineering", *Materials* 13, no. 24: 5815, 2015, doi: 10.3390/ma13245815
- [32] A. Phinyomark, P. Phukpattaranont, and C. Limsakul, "Feature reduction and selection for EMG signal classification", *Expert systems with applications*, 39(8), 7420-7431, 2012, doi: 10.1016/j.eswa.2012.01.102.
- [33] F. Yinfeng et al, "A multichannel surface EMG system for hand motion recognition", *Int J Humanoid Rob* 12:381-509, 2015, doi: 10.1142/S0219843615500115
- [34] M. Saranya, R. Kiruba, K. Srinivasan, T. A. Sanju, T. J. J. Antony and M. A. Kumar, "A Framework for Enhancing Cutting Edge Smart Assistive Technologies to Hemiparesis Patients," 2024 Second International Conference on Intelligent Cyber Physical Systems and Internet of Things (ICoICI), Coimbatore, India, 2024, pp. 986-992, doi: 10.1109/ICoICI62503.2024.10696094.
- [35] D. Roman-Liu, and P. Bartuzi, "Influence of type of MVC test on electromyography measures of biceps brachii and triceps brachii", *International journal of occupational safety and ergonomics*, 24(2), 200-206, 2018, doi: 10.1080/10803548.2017.1353321
- [36] G. Li, D. Bai, G. Jiang, D. Jiang, J. Yun, Z. Yang, and Y. Sun, "Continuous dynamic gesture recognition using surface EMG signals based on blockchain-enabled internet of medical things", *Information Sciences*, 646, 119409, 2023, doi: 10.1016/j.ins.2023.119409.
- [37] G. Yu, Z. Deng, Z., Bao, Y. Zhang, B. He, "Gesture Classification in Electromyography Signals for Real-Time Prosthetic Hand Control Using a Convolutional Neural Network-Enhanced Channel Attention Model". *Bioengineering*. 10(11):1324, 2023, doi: 10.3390/bioengineering10111324.
- [38] L. H. Smith, L. J. Hargrove, B. A. Lock and T. A. Kuiken, "Determining the Optimal Window Length for Pattern Recognition-Based Myoelectric Control: Balancing the Competing Effects of Classification Error and Controller Delay," in *IEEE Transactions on Neural Systems and Rehabilitation Engineering*, vol. 19, no. 2, pp. 186-192, April 2011, doi: 10.1109/TNSRE.2010.2100828.